EUROPEAN ORGANIZATION FOR NUCLEAR RESEARCH

Proposal to the ISOLDE and Neutron Time-of-Flight Committee

Exploring octupole collectivity in neutron-rich $A = 217 - 226$ astatine and radon nuclei, using decay-tagged in-source laser spectroscopy.

October 2, 2024

A. N. Andreyev[1], O. Ahmad[2], A. Ajayakumar[3], B. Andel[4], S. Antalic[4], M. Au[3], J. Benito[5], C. Bernerd[3], K. Blaum[6], M. J. G. Borge[7], K. Chrysalidis[3], T. E. Cocolios[2], J. G. Cubiss[1,8], T. Day Goodacre[9], L. P. Gaffney[10], G. Georgiev[11], P. F. Giesel[12], C. Fajardo[2], V. N. Fedosseev[3], K. Flanagan[9], L. M. Fraile[5], R. Heinke[9], A. Illana[5], U. Köster[13], D. Lange[6], R. Lica[14], D. Lunney[15], K. M. Lynch[9], D. McElroy [9], A. McFarlane[1], A. McGlone[9], C. Mihai[14], J. Mišt[4], L. Nies[3], Ch. Schweiger[6], L. Schweikhard[12], C. Page[1], J. R. Reilly[3], R. E. Rossel[3], S. Rothe[3], M. Scheck[16], J. Warbinek[3], J. W. Wessolek[3,9], J. Wilson[1], J. L. Wood[17], Z. Yue[1,3]
+ IDS Collaboration

[1]*School of Physics, Engineering and Technology, University of York, York, YO10 5DD, U.K.*
[2]*KU Leuven, Instituut voor Kern- en Stralingsfysica, B-3001 Leuven, Belgium*
[3]*CERN, CH-1211 Geneva 23, Switzerland*
[4]*Comenius University in Bratislava, Bratislava, Slovakia*
[5]*Grupo de Fìsica Nuclear & IPARCOS, Universidad Complutense de Madrid, Madrid, Spain*
[6]*Max-Planck-Institute for Nuclear Physics, Heidelberg, Germany*
[7]*Instituto de Estructura de la Materia, CSIC, E-28006 Madrid, Spain*
[8]*School of Physics and Astronomy, University of Edinburgh, Edinburgh, EH9 3FD, U.K.*
[9]*Department of Physics, University of Manchester, Manchester, U.K.*
[10]*University of Liverpool, Liverpool, U.K.*
[11]*IJCLab/CNRS, Université Paris-Saclay, France*
[12]*Universität Greifswald, Germany*
[13]*ILL, Grenoble, France*
[14]*Horia Hulubei National Institute for Physics and Nuclear Engineering, RO-077125 Bucharest, Romania*
[15]*CNRS/Universite Paris-Saclay, France*
[16]*University of the West of Scotland, Paisley, U.K.*
[17]*School of Physics, Georgia Institute of Technology, Atlanta, GA 30332, U.S.A.*

CERN-INTC-2024-068 / INTC-P-720
02/10/2024

Spokesperson: [James Cubiss] [james.cubiss@cern.ch],
[Andrei Andreyev] [andrei.andreyev@york.ac.uk],
[Daniel Lange] [daniel.lange@cern.ch].
Contact person: [Katerina Chrysalidis] [kchrysal@cern.ch]

Abstract: We propose to study neutron-rich $^{217-226}$At using high-resolution in-source laser spectroscopy, and the excited levels in $^{223-226}$Rn by decay spectroscopy of the laser ionised astatine precursors. The electromagnetic moments and the changes in the mean-squared charge radii will be used to investigate the onset of quadrupole and octupole collectivity in the ground and isomeric states of the isotopes $^{217-226}$At. The results will delineate the lower border of the region where octupole deformation is expected. The data will be used to test the predictions from cutting edge density functional theory. At the same time, $\beta - \gamma$ spectroscopy will be used to study the structures of the radon decay daughters.

Requested shifts: [24] shifts, (split into [1] runs over [1] years)

1 Introduction

An intriguing feature of the atomic nucleus is its ability to minimise its energy by adopting deformed shapes. In recent years, the discovery of exotic permanent octupole deformations (i.e. pear shapes) [1] has been of interest for nuclear structure studies [2], as well as for searches for sources of new physics beyond the Standard Model [3]. In particular, odd-A atoms containing such pear-shaped nuclei are prime candidates in the search for enhanced permanent electric dipole moments, through the interaction between atomic electrons and the nuclear Schiff moment [4, 5, 6].

Octupole shapes are expected in regions of the nuclear chart where single-particle configurations with $\Delta\ell = \Delta j = 3$ lie close together at the Fermi surface. The nuclei north-east of ^{208}Pb with $Z \sim 88$, $N \sim 134$ inhabit one such region. Here, correlations between particles occupying the $\pi 2f_{7/2}$ and $\pi 1i_{13/2}$ proton states, and the $\nu 2g_{9/2}$ and $\nu 1j_{15/2}$ neutron orbitals, drive octupole collectivity [see Fig. 1(a)]. However, it is only recently that beams of isotopes with $Z \sim 88$, $N \sim 134$ have become available with high enough intensities to perform precision studies [1, 7].

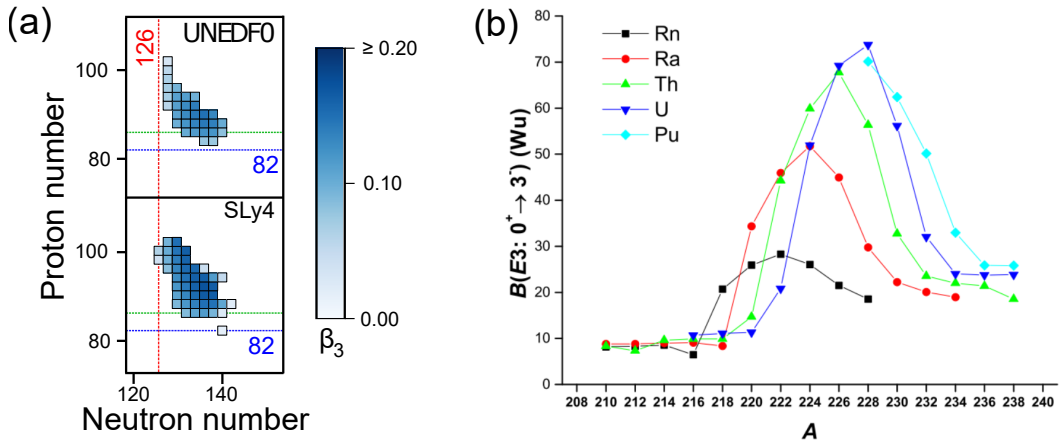

Figure 1: Calculations for the (a) ground state octupole deformation parameter, β_3 (adapted from [8]), and (b) electric octupole transition strengths $B(E3; 0^+ \rightarrow 3^-)$ [9] of even-even nuclei North-East of ^{208}Pb. The green lines in panel (a) indicate the position of the radon ($Z = 86$) isotopes.

The experimental signatures for octupole correlations include enhanced electric octupole transition strengths [$B(E3)$s, calculations for which are shown in Fig. 1(b)], and the presence of near-degenerate, parity-doublet bands in odd-A nuclei, or interleaving opposite parity bands in even-even cases [2]. Complementary to these are nuclear electromagnetic moments and changes in the mean-squared charge radii ($\delta\langle r^2\rangle$). For the former, the magnetic dipole moment (μ) provides an insight into the underlying configuration of valence particles, and hence is sensitive to the mixing between states of different parities, which is possible in the presence of octupole deformations [10]. Meanwhile, an inverted odd-even staggering (OES) in $\delta\langle r^2\rangle$ values — whereby the $\delta\langle r^2\rangle$ value of an odd-N isotope is *greater* than the average of its even-N neighbours — is observed in nuclei inhabiting regions where octupole collectivity is expected [11, 12, 13].

2 Physics case

2.1 Previous work on neutron-rich astatine and radon isotopes

The neutron-rich astatine ($Z = 85$) and radon ($Z = 86$) isotopes lie on the border of the predicted octupole region [see Fig. 1(a)]. Therefore, the properties of the ground states and low-lying structures in these isotopes are key for delineating the octupole region and constraining models that attempt to describe this behaviour.

Historically, studies of these nuclides at ISOLDE have been hindered by the presence of strong, isobaric contamination from surface ionised francium and radium. Our recent laser spectroscopy results are the only published $\delta\langle r^2\rangle$, μ and electric quadrupole moment (Q) values for neutron-rich astatine isotopes [14], but were limited to ^{217,218,219}At due to the aforementioned contamination. Our data revealed that the μ and I^π of ^{217,219}At are consistent with $\pi 1h_{9/2}$ configurations expected from the spherical shell model. Similarly, their low-lying structures are well described by a $\pi 1h_{9/2}$ seniority scheme. However, $\mu(^{218}\text{At})$ could not be described by the additivity rule using the expected $\pi 1h_{9/2} \otimes \nu 2g_{9/2}$ configuration, but could be explained by including an admixture from $\pi 1i_{13/2}$. This admixture between states of opposite parity is only possible with the presence of octupole collectivity, and could suggest that the odd-odd astatine isotopes exhibit octupole correlations. It is therefore important to extend the current data to the $A \sim 224$ region where octupole collectivity is expected to be strongest (see Fig. 1).

Additionally, a large OES inversion in $\delta\langle r^2\rangle$ was observed, with $\delta\langle r^2\rangle(^{218}\text{At})$ being larger than the average of neighbouring ^{217,219}At [see Fig. 2(a)]. The degree of this inversion, quantified by the OES parameter ($\gamma_N = 2\delta\langle r^2\rangle_{N-1,N}/\delta\langle r^2\rangle_{N-1,N+1}$), shows a stronger inversion in astatine relative to the nearby radon and francium chains at the same neutron number [$N = 133$, see Fig. 2(b)]. Our $\gamma_N(^{218}\text{At})$ was well described by the presence of quadrupole-octupole collectivity, with an octupole deformation of $|\beta_3| \sim 0.1$ taken from Ref. [15].

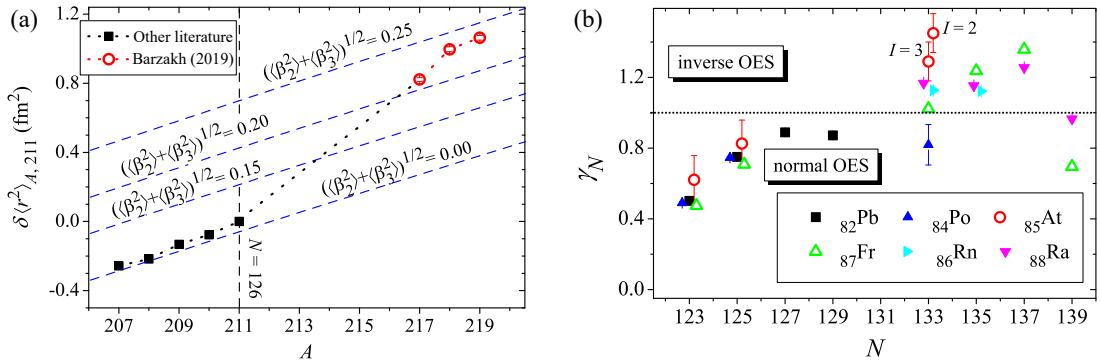

Figure 2: (a) The changes in mean-squared charge radii of astatine isotopes and (b) the OES parameter for different isotopes in the vicinity of $N = 126$, as a function of the neutron number. A value of $\gamma_N > 1$ indicates an inversion of the OES. Figures adapted from Ref. [14]. The two data points for ^{218}At represent the results for two different spin assumptions, $I = 2$ or 3.

As well as the μ and $\delta\langle r^2\rangle$ values, the Q provides additional constraints for the nuclear

models and gives insight into the degree of quadrupole collectivity, which is expected to increase with neutron number. Although Q values were determined for $^{217-219}$At in our previous work [14], the precision ($\approx 20-50\%$) was not sufficient to make firm conclusions on the level of quadrupole deformation.

As for the radon isotopes, the low-lying structures of the even-A $^{220-226}$Rn are reasonably well known, apart from ^{226}Rn, for which a partial level scheme was only recently constructed [7]. However, the study was unable to identify the $I^\pi = 1^-$ and 3^- members of the octupole bands, the energies of which are of key importance. Nevertheless, in Ref. [7] it was found that the even-even isotopes $^{222-226}$Rn likely have vibrational rather than static octupole deformations. This is consistent with the calculations shown in Fig. 1 which show the radon isotopes to have smaller β_3 and $B(E3)$ values than the higher-Z isotopes, and hence are softer to octupole degrees of freedom.

Contrastingly, very little is known about the low-lying structures of the odd-A isotopes $^{221-225}$Rn, other than the ground-state properties from laser-spectroscopy measurements [12, 16], and the first excited state in ^{221}Rn from an α-decay study of ^{225}Ra [17]. However, particle-asymmetric rotor models suggest that the ordering of the low-lying states in these nuclei is particularly sensitive to the presence of octupole deformation (see Fig. 4 in Ref. [18]). Indeed, in Ref. [18] it was noted that the ground states of ^{221,223,225}Rn appeared to have complex structures, and that replicating the experimental I^π, μ and Q values was a significant challenge that required additional information from experiment.

2.2 Proposed measurements

2.2.1 Octupole collectivity in neutron-rich astatine

The results presented in Fig. 2 were taken using RILIS in its narrowband mode of operation [14], using the ionisation scheme shown in Fig. 3(a). Isotope shift (IS) and hyperfine structure (hfs) measurements performed on the 795.21 nm transition, where a linewidth of ≈ 1 GHz was achieved.

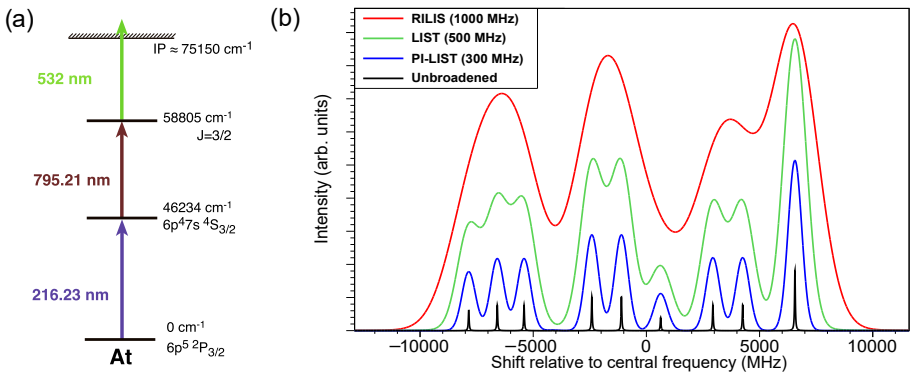

Figure 3: The (a) three-step resonance ionisation scheme that will be used, and (b) comparison of simulations of the hfs spectra expected from scanning the 795.21 nm transition for a $I = 9/2$ nucleus, recorded in normal RILIS mode (red) [14], LIST mode (green), and PI-LIST mode (blue). The vertical black lines represent the unbroadened hyperfine transitions, with their heights indicating the relative intensities.

We propose to extend the $\delta\langle r^2\rangle$ measurements along the chain of neutron-rich astatine isotopes to confirm whether the inverted OES extends to the heavier masses. We will use a UC_x target combined with the Laser Ion Source and Trap (LIST) to suppress surface-ionised isobaric francium beam contaminant, with only a factor of ≈ 30 reduction in the extraction of the isotopes of interest [19]. For $^{218-224}$At, the expected yields are large enough to operate in perpendicularly-illuminated LIST (PI-LIST) mode, which has a reduction in efficiency of < 500 relative to normal RILIS operation. However, the PI-LIST can achieve linewidths of 100-300 MHz allowing Q values to be extracted. It was also shown during the IS664 experiment that by running the LIST in normal mode, improved resolutions of ~ 500 MHz were achievable using a pulsed amplified Ti:Sa ring cavity seeded with a high-resolution continuous wave laser from the CRIS setup. This will give access to Q values for more weakly produced cases, albeit at lower precision.
With the improved resolution, the limiting factor on our results will be the uncertainties related to available atomic data and calculations. With the available data, our extracted Q values would have a $\sim 50\%$ uncertainty due to systematics stemming from calculations of the hyperfine parameters (a and b) of the atomic ground state in astatine (10%), and from the experimental b_0/b_1 ratio between the ground and first excited state quadrupole parameters (40%). Therefore, we will perform additional scans of the 216.23 nm transition for strongly produced ^{200}At ($I^\pi = 3$, 7 and 10) and ^{211}At ($I^\pi = 9/2^-$) using the PI-LIST, to accurately determine these atomic factors. This will allow a precision of $< 15\%$ in Q values extracted from the measurements, as well as new information to be extracted from our previous data.

2.2.2 Low-lying structures and octupole collectivity in neutron-rich radon isotopes

In parallel to the primary IS/hfs study on astatine, we will perform decay measurements to explore the excited state structures in $^{220-226}$Rn. The β-decay schemes for the precursor astatine isotopes are completely unknown, apart from that of ^{220}At shown in Fig. 4. Furthermore, having only been observed to pass through the FRS recoil separator, no spectroscopic information is known for ^{225,226}At and only lower limits of $T_{1/2} > 300$ ns are known for their half-lives. Hence, the data we will collect would provide the first ever information on these two very exotic cases.

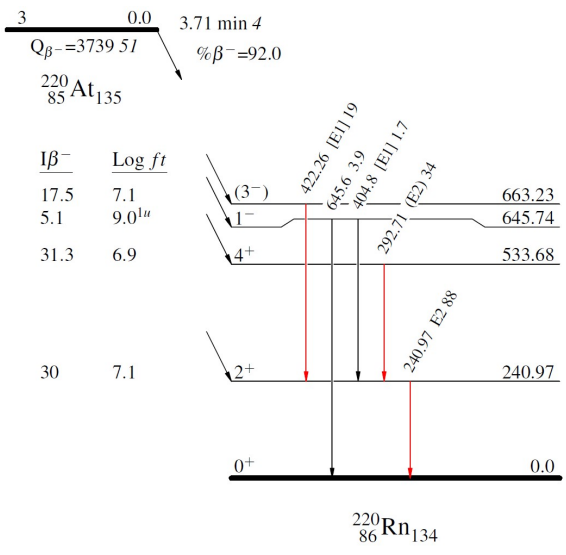

Figure 4: The β-decay scheme for ^{220}At$\rightarrow$ ^{220}Rn taken from [20, 21, 22].

The high γ-detection efficiency ($\sim$5% at 1 MeV) of the IDS germanium clover detectors will be combined with plastic scintillators for β tagging and an annular silicon detector at the implantation position. Ancillary arrays of LaBr detectors for fast-timing measurements and silicon detectors for conversion electron spectroscopy positioned at a

secondary decay station below the implantation position will also be used. This will allow detailed decay schemes to be constructed, including information on excitation energies, $T_{1/2}$, I^π, γ-ray intensities and conversion coefficients. In particular, the even-A astatine isotopes have, or are expected to have ground states of $I^\pi = 2^-, 3^-$. The β decay of these ground states should strongly populate the $I^\pi = 1^-$ and 3^- members of the octupole and the $I^\pi = 2^+$ and 4^+ of the ground state bands in the even-A radon isotopes. An example of this is shown in the β-decay scheme for ^{220}At in Fig. 4, with 17.5% and 5.1% feeding to the $I^\pi = 3^-$ and 1^- states, respectively. By measuring the lifetimes and branching ratios of the decays from the $I^\pi = 3^-$ states we will be able to directly determine $B(E3)$ values. For the most intensely produced cases, these data will be collected during the astatine IS and hfs scanning. However, we request three shifts for dedicated decay measurements of the more weakly produced $^{223-226}$At.

3 Method

The hfs spectra will be measured using the ISOLDE Decay Station (IDS) to record the number of characteristic decays, or the ISOLTRAP MR-ToF-MS to count ions, as a function of the laser frequency of the scanned transition. The scanning resolution compared to our previous measurements will be optimised by using a pulsed amplified Ti:Sa ring cavity seeded with continuous wave laser light which will be generated at the CRIS installation and delivered to RILIS via a fibre link.

An annular silicon detector will be used at IDS for α detection ($\approx 15\%$ efficiency), whilst plastic scintillators and germanium detectors will be used for measuring β and γ radiation, respectively. The expected peak γ-ray detection efficiency of IDS is $\approx 17\%$ at the implantation position, for 200 keV γ rays. In addition we plan to use a secondary decay measurement chamber ($\approx 15\%$ peak γ and 50% β detection efficiency) between the implantation point and the IDS tape station. Here, IDS clover detectors will be combined with LaBr and plastic scintillators to perform lifetime measurements of excited states in neutron-rich daughter radon isotopes, and provide additional efficiency for constructing hfs spectra through decay counting of long-lived and daughter activities. In the past, this approach allowed IS and hfs measurements to be performed with implantation rates as low as 0.01 ions/s.

Figure 5 summarises the yields estimates for the astatine isotopes, made using our data for ^{217,218}At in Ref. [14], and conservative values for the in-target production yields simulated by ABRABLA, available through the ISOLDE yield database [23, 24]. The number of shifts accounts for the $T_{1/2}$ and respective yields of each isotope, as well as the reduction in the yields in the LIST and PI-LIST modes, relative to normal RILIS operation. A loss factor of 30 is assumed for operation using the LIST, and a conservative factor of 500 when using PI-LIST mode [19].

Yield estimates:

Yields for astatine isotopes of mass A were calculated using the expression [25]:

$$Y(A) = Y(218)\frac{P(A)}{P(218)}\Big(\frac{T_{1/2}(A)}{T_{1/2}(218)}\Big)^{\alpha} \quad (1)$$

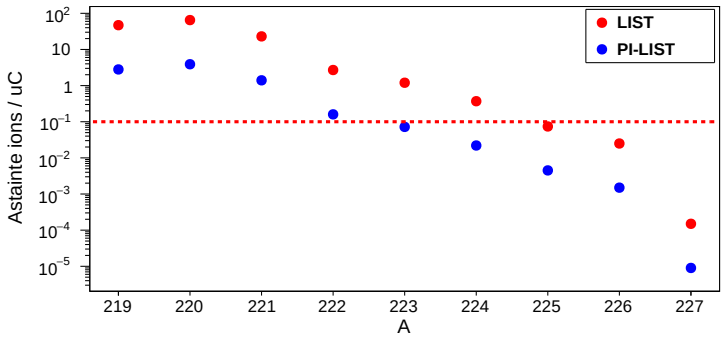

Figure 5: The calculated yields for isotopes of astatine based on our previous data from [14] and conservative in-target calculations ABRABLA. The red and blue data points are estimates for operating the target in LIST and PI-LIST mode, respectively. The dashed red line is the approximate limit of sensitivity for IDS.

where $Y(218)$ was the yield measured for ^{218}At in Ref. [14] (90 ions/μC), and $P(A)$ and $T_{1/2}(A)$ are the in-target production and half-life for the isotope of mass A, respectively. A value of $\alpha = 0.89$ taken from Ref. [25] was used in our yield calculations, which are shown in Fig. 5.

Summary of requested shifts: Based on our previous data and the yield estimates, **we request 18 shifts for the IS and hfs measurements**, which are summarised in Table 1. This will allow us to make measurements up to ^{224}At in PI-LIST mode, and ^{225,226}At in LIST mode. We request a further **3 shifts** dedicated to decay measurements for exploring the low-lying structures in radon isotopes. In addition to this we request one extra day for setup of the lasers and beam tuning to IDS and ISOLTRAP (**3 shifts**). This is to account for the additional challenges associated with beam tuning from a LIST ion source in different operation modes. Therefore, we request a **total of 24 shifts**.

Table 1: Summary of requested shifts for laser scanning.

A	$T_{1/2}$	Scanning mode	New measurements	Shifts
200	6.92 s	PI-LIST	atomic factors	2.5
205	26.9 mins	PI-LIST	reference	1
211	7.2 hrs	PI-LIST	atomic factors	2.5
217	32.3 ms	PI-LIST	improved Q	1
218	1.5 s	PI-LIST	I, improved Q	1
219	56 s	PI-LIST	improved Q	1
220	3.71 mins	PI-LIST	I, $\delta\langle r^2\rangle$, μ, Q	1
221	2.3 mins	PI-LIST	I, $\delta\langle r^2\rangle$, μ, Q	1
222	54 s	PI-LIST	I, $\delta\langle r^2\rangle$, μ, Q	1
223	50 s	PI-LIST	I, $\delta\langle r^2\rangle$, μ, Q	1.5
224	1.3 mins	LIST/PI-LIST	I, $\delta\langle r^2\rangle$, μ, Q	1.5
225	$>$ 300 ns	LIST	I, $\delta\langle r^2\rangle$, μ, Q	1.5
226	$>$ 300 ns	LIST	I, $\delta\langle r^2\rangle$, μ, Q	1.5
			Total:	**18**

References

[1] L. P. Gaffney, P. A. Butler, M. Scheck, A. B. Hayes, F. Wenander, M. Albers, B. Bastin, C. Bauer, A. Blazhev, S. Bönig, N. Bree, J. Cederkäll, T. Chupp, D. Cline, T. E. Cocolios, T. Davinson, H. De Witte, J. Diriken, T. Grahn, A. Herzan, M. Huyse, D. G. Jenkins, D. T. Joss, N. Kesteloot, J Konki, M Kowalczyk, Th. Kröll, E. Kwan, R. Lutter, K. Moschner, P. Napiorkowski, J. Pakarinen, M. Pfeiffer, D. Radeck, P. Reiter, K. Reynders, S. V. Rigby, L. M. Robledo, M. Rudigier, S. Sambi, M. Seidlitz, B. Siebeck, T. Stora, P. Thoele, P. Van Duppen, M. J. Vermeulen, M. von Schmid, D. Voulot, N. Warr, K. Wimmer, K. Wrzosek-Lipska, C. Y. Wu, and M. Zielinska. Studies of pear-shaped nuclei using accelerated radioactive beams. *Nature*, 497(7448):199–204, may 2013.

[2] P. A. Butler and W. Nazarewicz. Intrinsic reflection asymmetry in atomic nuclei. *Reviews of Modern Physics*, 68(2):349–421, apr 1996.

[3] R. F. Garcia Ruiz, R. Berger, J. Billowes, C. L. Binnersley, M. L. Bissell, A. A. Breier, A. J. Brinson, K. Chrysalidis, T. E. Cocolios, B. S. Cooper, K. T. Flanagan, T. F. Giesen, R. P. de Groote, S. Franchoo, F. P. Gustafsson, T. A. Isaev, Á. Koszorús, G. Neyens, H. A. Perrett, C. M. Ricketts, S. Rothe, L. Schweikhard, A. R. Vernon, K. D. A. Wendt, F. Wienholtz, S. G. Wilkins, and X. F. Yang. Spectroscopy of short-lived radioactive molecules. *Nature*, 581(7809):396–400, may 2020.

[4] L. I. Schiff. Measurability of Nuclear Electric Dipole Moments. *Physical Review*, 132(5):2194–2200, dec 1963.

[5] Jacek Dobaczewski, Jonathan Engel, Markus Kortelainen, and Pierre Becker. Correlating Schiff Moments in the Light Actinides with Octupole Moments. *Physical Review Letters*, 121(23):232501, dec 2018.

[6] V. V. Flambaum and H. Feldmeier. Enhanced nuclear Schiff moment in stable and metastable nuclei. *Physical Review C*, 101(1):015502, jan 2020.

[7] P. A. Butler, L. P. Gaffney, P. Spagnoletti, J. Konki, M. Scheck, J. F. Smith, K. Abrahams, M. Bowry, J. Cederkäll, T. Chupp, G. de Angelis, H. De Witte, P. E. Garrett, A. Goldkuhle, C. Henrich, A. Illana, K. Johnston, D. T. Joss, J. M. Keatings, N. A. Kelly, M. Komorowska, T. Kröll, M. Lozano, B. S. Nara Singh, D. O'Donnell, J. Ojala, R. D. Page, L. G. Pedersen, C. Raison, P. Reiter, J. A. Rodriguez, D. Rosiak, S. Rothe, T. M. Shneidman, B. Siebeck, M. Seidlitz, J. Sinclair, M. Stryjczyk, P. Van Duppen, S. Vinals, V. Virtanen, N. Warr, K. Wrzosek-Lipska, and M. Zielinska. The observation of vibrating pear-shapes in radon nuclei. *Nature Communications*, 10(1):2473, jun 2019.

[8] Yuchen Cao, S. E. Agbemava, A. V. Afanasjev, W. Nazarewicz, and E. Olsen. Landscape of pear-shaped even-even nuclei. *Phys. Rev. C*, 102:024311, Aug 2020.

[9] P A Butler. Octupole collectivity in nuclei. *Journal of Physics G: Nuclear and Particle Physics*, 43(7):073002, jun 2016.

[10] E. Verstraelen, A. Teigelhöfer, W. Ryssens, F. Ames, A. Barzakh, M. Bender, R. Ferrer, S. Goriely, P. H. Heenen, M. Huyse, P. Kunz, J. Lassen, V. Manea, S. Raeder, and P. Van Duppen. Search for octupole-deformed actinium isotopes using resonance ionization spectroscopy. *Physical Review C*, 100(4):044321, 2019.

[11] A. Coc, C. Thibault, F. Touchard, H. T. Duong, P. Juncar, S. Liberman, J. Pinard, M. Carre, J. Lerme, J. L. Vialle, S. Buttgenbach, A. C. Mueller, and A. Pesnelle. Isotope shifts, spins and hyperfine structures of ^{118,146}Cs and of some francium isotopes. *Nuclear Physics, Section A*, 468(1):1–10, 1987.

[12] W. Borchers, R. Neugart, E. W. Otten, H. T. Duong, G. Ulm, and K. Wendt. Hyperfine structure and isotope shift investigations in $^{202–222}$Rn for the study of nuclear structure beyond Z=82. *Hyperfine Interactions*, 34(1-4):25–29, mar 1987.

[13] S. A. Ahmad, W. Klempt, R. Neugart, E. W. Otten, P. G. Reinhard, G. Ulm, and K. Wendt. Mean square charge radii of radium isotopes and octupole deformation in the 220-228 Ra region. *Nuclear Physics, Section A*, 483(2):244–268, jun 1988.

[14] A. E. Barzakh, J. G. Cubiss, A. N. Andreyev, M. D. Seliverstov, B. Andel, S. Antalic, P. Ascher, D. Atanasov, D. Beck, J. Bieroń, K. Blaum, Ch Borgmann, M. Breitenfeldt, L. Capponi, T. E. Cocolios, T. Day Goodacre, X. Derkx, H. De Witte, J. Elseviers, D. V. Fedorov, V. N. Fedosseev, S. Fritzsche, L. P. Gaffney, S. George, L. Ghys, F. P. Heßberger, M. Huyse, N. Imai, Z. Kalaninová, D. Kisler, U. Köster, M. Kowalska, S. Kreim, J. F. W. Lane, V. Liberati, D. Lunney, K. M. Lynch, V. Manea, B. A. Marsh, S. Mitsuoka, P. L. Molkanov, Y. Nagame, D. Neidherr, K. Nishio, S. Ota, D. Pauwels, L. Popescu, D. Radulov, E. Rapisarda, J. P. Revill, M. Rosenbusch, R. E. Rossel, S. Rothe, K. Sandhu, L. Schweikhard, S. Sels, V. L. Truesdale, C. Van Beveren, P. Van Den Bergh, P. Van Duppen, Y. Wakabayashi, K. D. A. Wendt, F. Wienholtz, B. W. Whitmore, G. L. Wilson, R. N. Wolf, and K. Zuber. Inverse odd-even staggering in nuclear charge radii and possible octupole collectivity in ^{217,218,219}At revealed by in-source laser spectroscopy. *Physical Review C*, 99(5):054317, 2019.

[15] P. Möller, R. Bengtsson, B.G. Carlsson, P. Olivius, T. Ichikawa, H. Sagawa, and A. Iwamoto. Axial and reflection asymmetry of the nuclear ground state. *Atomic Data and Nuclear Data Tables*, 94(5):758–780, sep 2008.

[16] R. Neugart, E. Arnold, W. Borchers, W. Neu, G. Ulm, and K. Wendt. New techniques and results of collinear laser spectroscopy radon, xenon and holmium. In *AIP Conference Proceedings*, volume 164, pages 126–135. AIP, 1987.

[17] C. F. Liang, P. Paris, and R. K. Sheline. α decay of ^{225}Ra. *Physical Review C*, 62(4):047303, sep 2000.

[18] G. A. Leander and Y. S. Chen. Reflection-asymmetric rotor model of odd A$\sim$219-229 nuclei. *Phys. Rev. C*, 37:2744–2778, Jun 1988.

[19] Reinhard Heinke, Mia Au, Cyril Bernerd, Katerina Chrysalidis, Thomas E. Cocolios, Valentin N. Fedosseev, Isabel Hendriks, Asar A.H. Jaradat, Magdalena Kaja, Tom

Kieck, Tobias Kron, Ralitsa Mancheva, Bruce A. Marsh, Stefano Marzari, Sebastian Raeder, Sebastian Rothe, Dominik Studer, Felix Weber, and Klaus Wendt. First on-line application of the high-resolution spectroscopy laser ion source PI-LIST at ISOLDE. *Nuclear Instruments and Methods in Physics Research Section B: Beam Interactions with Materials and Atoms*, 541:8–12, 2023.

[20] NNDC. *Evaluated Nuclear Structure Data File*, 2024.

[21] C F Liang, P Paris, E Ruchowska, and C Briancon. A new isotope 85220at135. *Journal of Physics G: Nuclear and Particle Physics*, 15(3):L31, mar 1989.

[22] D. G. Burke, H. Folger, H. Gabelmann, E. Hagebø, P. Hill, P. Hoff, O. Jonsson, N. Kaffrell, W. Kurcewicz, G. Løvhøiden, K. Nybø, G. Nyman, H. Ravn, K. Riisager, J. Rogowski, K. Steffensen, and T. F. Thorsteinsen. New neutron-rich isotopes of astatine and bismuth. *Zeitschrift für Physik A Atomic Nuclei*, 333(2):131–135, jun 1989.

[23] The ISOLDE yield database, version 0.2. `https://cern.ch/isolde-yields`, 2021. [Online; accessed 01.04.2023].

[24] J. Ballof, J.P. Ramos, A. Molander, K. Johnston, S. Rothe, T. Stora, and Ch.E. Düllman. The upgraded ISOLDE yield database - a new tool to predict beam intensities. *Nuclear Instruments and Methods in Physics Research Section B: Beam Interactions with Materials and Atoms*, 463:211–215, 2020.

[25] S. Lukić, F. Gevaert, A. Kelić, M.V. Ricciardi, K.-H. Schmidt, and O. Yordanov. Systematic comparison of isolde-sc yields with calculated in-target production rates. *Nuclear Instruments and Methods in Physics Research Section A: Accelerators, Spectrometers, Detectors and Associated Equipment*, 565(2):784–800, 2006.

4 Details for the Technical Advisory Committee

4.1 General information

Describe the setup which will be used for the measurement. If necessary, copy the list for each setup used.

☒ Permanent ISOLDE setup: *IDS, ISOLTRAP, RILIS*

- ☒ To be used without any modification
- ☐ To be modified: *Short description of required modifications.*

☐ Travelling setup (*Contact the ISOLDE physics coordinator with details.*)

- ☐ Existing setup, used previously at ISOLDE: *Specify name and IS-number(s)*
- ☐ Existing setup, not yet used at ISOLDE: *Short description*
- ☐ New setup: *Short description*

4.2 Beam production

For any inquiries related to this matter, reach out to the target team and/or RILIS (please do not wait until the last minute!). For Letters of Intent focusing on element (or isotope) specific beam development, this section can be filled in more loosely.

- Requested beams:

Isotope	Production yield in focal point of the separator ($/\mu$C)	Minimum required rate at experiment (pps)	$T_{1/2}$
^{200}At	$> 10^3$	0.2	>6 s
^{205}At	$> 10^6$	0.2	26.9 mins
^{211}At	$> 10^6$	0.2	7.2 hrs
$^{217-226}$At	$10^{-1} - 10^3$	0.2	>1 s

- Full reference of yield information: *Yields recorded during IS534 and extrapolations from yield database, scaled to measured yields*
- Target - ion source combination: *UC_x + LIST*
- RILIS? *Yes*
  - ☒ Special requirements: *isomer selectivity, LIST, PI-LIST, ultra-narrow bandwidth laser scanning using an injection-seeded laser, fibre transport of CW laser light from CRIS, laser shutter access, etc.*
- Expected contaminants: *Surface ionised Fr*
- Acceptable level of contaminants: *Not sensitive to stable contaminants. The LIST will suppress most of the surface ionised contamination as seen in LOI219 (10^6 suppression), the selectivity of IDS and ISOLTRAP can easily deal with any remaining contamination.*

- Can the experiment accept molecular beams? *No*
- Are there any potential synergies (same element/isotope) with other proposals and LOIs that you are aware of? *INTC-I-158*

4.3 Shift breakdown

The beam request only includes the shifts requiring radioactive beam, but, for practical purposes, an overview of all the shifts is requested here. Don't forget to include:

- Isotopes/isomers for which the yield need to be determined
- Shifts requiring stable beam (indicate which isotopes, if important) for setup, calibration, etc. Also include if stable beam from the REX-EBIS is required.

An example can be found below, please adapt to your needs. Copy the table if the beam time request is split over several runs.

Summary of requested shifts:

With protons	Requested shifts
^{200}At, scans to improve accuracy of atomic factors	4
^{205}At, hfs reference scans	1
$^{217-226}$At, data taking, hfs scans	13
$^{217-226}$At, data taking, decay measurements	3
Without protons	Requested shifts
Stable beam to setups	3

4.4 Health, Safety and Environmental aspects

4.4.1 Radiation Protection

- If radioactive sources are required:
  - Purpose? *Energy and efficiency calibrations of detectors.*
  - Isotopic composition? ^{137}Cs, ^{241}Am, ^{152}Eu, ^{133}Ba, ^{60}Co, *quadruple* α *source*
  - Activity? < 300 *kBq, ISO standard calibration sources.*
  - Sealed/unsealed? *both*
- For collections:
  - Number of samples? *None*
  - Activity/atoms implanted per sample? *n/a*
  - Post-collection activities? *n/a*